All-optical poling in polymers: dynamical aspects and perspectives

Pure Appl. Opt. **7** (1998) 141–150. Printed in the UK PII: S0963-9659(98)88364-5

All-optical poling in polymers: dynamical aspects and perspectives

Jean-Michel Nunzi, Céline Fiorini, Anne-Catherine Etilé and François Kajzar

LETI, CEA Technologies Avancées, DEIN-SPE, Groupe Composants Organiques, CEA/Saclay, 91191 Gif-sur-Yvette Cedex, France

Received 21 October 1997

Abstract. All-optical poling is based on the excitation of nonlinear molecules using dual-frequency beams. The process is optimized at a molecular level when the molecules are resonantly excited. From the point of view of frequency conversion applications, this raises the question of device transparency to the frequency-converted output. In order to treat this efficiency transparency tradeoff, we recently developed a simple model accounting for all the observable parameters. The model permits a good prediction of the poling dynamics. Its self-consistency permits the description of all the known all-optical poling schemes. In particular, analysis of the parameters of the model permits the identification of new strategies towards the realization of stable and transparent phase-matched materials for frequency conversion. Some preliminary experimental results are presented in this respect.

1. Introduction

A key issue in the field of nonlinear optical polymers for second-order processes is the achievement of a non-centrosymmetric order. One challenging prospect is to achieve it by optical means in order to take full advantage of its rich processing capabilities. Indeed, the all-optical poling of polymers offers an interesting alternative to the realization of non-centrosymmetric structures. Of particular interest is the possibility to control extensively the spatial and tensorial properties of polymers using optical beams [1].

The optical induction of quasi-permanent birefringence and dichroism in azo-dye polymers has been the subject of many studies [2, 3]. At the microscopic level, the mechanism involves a selective axial excitation of the molecules which are aligned vertically or horizontally depending on the polarization direction of the incident beam. The orientational redistribution following each excitation–relaxation cycle leads to a quasi-permanent alignment of the dye molecules. Such a process does not lead to the induction of a macroscopic second-order property inside the medium because no polar order results from the application of a monochromatic light beam $E_\omega(t)$, even if this beam is polarized. Such field changes sign at frequencies as high as 10^{15} Hz, resulting in a zero temporal average $\langle E_\omega(t)\rangle_t$. However, those photo-induced alignment effects show that if a polar photoexcitation of the chromophores is possible, then a polar orientation should result.

A few years ago, experiments demonstrated that the coherent superposition of two beams at fundamental and second-harmonic (SH) frequencies could result in the breaking of the initial centrosymmetry of a medium [4]. Experimentally, it was shown that further to the simultaneous irradiation of a fibre with the coherent superposition of two beams at

0963-9659/98/020141+10$19.50

the fundamental and SH frequencies, an efficient SH generation occurred with a conversion efficiency of up to 10%. The so-called seeding process was identified by Baranova and Zel'dovich as a six-wave mixing effect [5]. The interference between a fundamental wave E_ω and its SH $E_{2\omega}$ leads to the presence of a polar field $E(t) = E_\omega(t) + E_{2\omega}(t)$ inside the medium. More precisely, it can be shown that the temporal average of the field cubed $\langle E^3(t)\rangle_t$, is non-zero. Thanks to coherent nonlinear interactions, it results in a polar selective excitation of the molecules oriented in a given direction and sense. The process leads finally to the recording of a $\chi^{(2)}$ susceptibility with a spatial period satisfying the phase-matching condition for SH generation (cf figure 1).

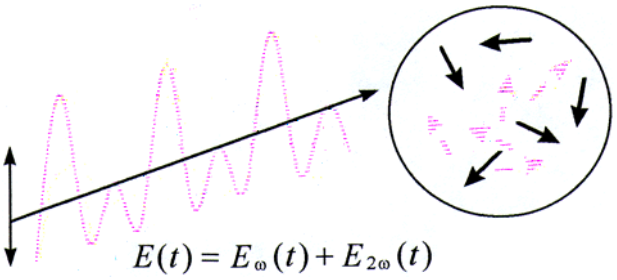

Figure 1. The polar interference between fundamental and harmonic waves induces a polar excitation in a centrosymmetric set of non-centrosymmetric molecules.

Using a six-wave mixing configuration in a picosecond regime, we have demonstrated for the first time the possibility of photo-inducing a transient second-order susceptibility $\chi^{(2)}$ in solutions of dye molecules [6, 7]. The physical origin of the effect was attributed to an orientation hole burning in the isotropic distribution of molecules. More recently, using spin-coated films of dyed polymers and copolymers, we have demonstrated for the first time the possibility of achieving an efficient and quasi-permanent poling of the molecules [8, 9]. The effect was attributed to a redistribution of the molecular orientations further to orientation hole burning.

Optimizing the preparation conditions [10], the same orientation efficiency as using the more standard corona poling method was achieved [9]. The influence of such 'seeding' parameters as the relative phase and relative intensities between the writing beams at ω and 2ω frequencies were clarified. The tensor properties of the induced $\chi^{(2)}$ susceptibility were also analysed and the mechanisms responsible for the permanent orientation of the molecules were identified. In this paper, we propose a simplified model which, based on three significant parameters, accounts for the essential physics relevant to the all-optical poling process and permits optimization of its efficiency. Predictions of the model are compared with the experiment. As an application, the all-optical poling of transparent polymers is presented.

2. All-optical poling dynamics: model

The macroscopic polarizability of an assembly of non-interacting molecules is obtained theoretically from the corresponding microscopic one after averaging over all possible orientations. For frequency doubling, the second-order susceptibility $\chi^{(2)}$ relates to the

molecular hyperpolarizability β through

$$\chi^{(2)}_{\Delta\Delta\Delta} = \int_{\Omega} N(\Omega)\,\beta_{\Delta\Delta\Delta}(\Omega)\,\mathrm{d}\Omega \tag{1}$$

where $N(\Omega)$ is the density of molecules oriented in a direction Ω and Δ is a given direction in the (x, y) plane of the film. We do not explicitly mention local field factors but they can be used. In order to describe $\chi^{(2)}$ growth and decay, we simply need a physical description of $N(\Omega)$. In every all-optical scheme, the dynamics of evolution of $N(\Omega)$ is governed by three terms (cf figure 2): first is the rate of optical excitation which creates polar orientation, second is the rate of non-radiative relaxation-induced transport which freezes the orientation and third is the rate of free diffusion which tends to restore the original equilibrium.

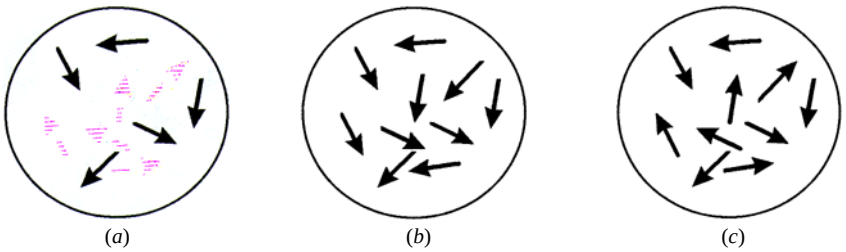

Figure 2. Effect of the all-optical poling on the evolution of $N(\Omega)$. (*a*) Molecules are initially excited with the polar field (as broken arrows). (*b*) Non-radiative relaxation induces a transport of orientation which freezes the polar orientation after relaxation (they point to the bottom). (*c*) Free diffusion tends to restore the original isotropic equilibrium.

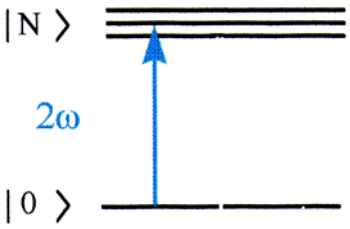

Figure 3. Simultaneous excitation of a single molecule through one (ω) and two-photon (2ω) excitations from the ground state $|0\rangle$ to excited states $|N\rangle$.

In the orientation hole-burning scheme, the first term is simply expressed as the rate of excitation of molecules undergoing simultaneous one and two-photon excitations from ground to excited states (cf figure 3).

For a non-centrosymmetric molecule, the orientation hole-burning term can be expressed as [11]

$$\left.\frac{\partial N(\Omega)}{\partial t}\right|_{HB} = \frac{-\mathrm{i}}{2\hbar}\left\langle \underline{\underline{\alpha}}\bar{E}\bar{E}^{*} + \underline{\underline{\underline{\beta}}}\bar{E}\bar{E}\bar{E}^{*} + \underline{\underline{\underline{\underline{\gamma}}}}\bar{E}\bar{E}^{*}\bar{E}\bar{E}^{*} + \text{higher orders}\right\rangle_{t} + \text{CC} \tag{2}$$

where CC represents the complex conjugate terms. It is the superposition of one, dual and two-photon absorptions in which α, β, γ are the microscopic polarizability tensors. Transformation matrices relating the molecule coordinates to the laboratory axis are implicit

in the tensorial products. So, polar excitation is proportional to the imaginary part of the microscopic polarizability β. After excitation, molecules decay back to the ground state. If decay is radiative, the excitation may be considered as lost. Otherwise, molecules with a typical 200 g molar mass which have to relax typically by 2 eV energy (visible excitation) undergo an equivalent heating of their rotation–vibration motion modes by $\Delta T \approx 10^3$ K. Such relaxation transports the molecules into a different orientation which strongly affects the original distribution. The excess temperature relaxes on a picosecond to second time scale, depending on the type of molecule (it is on a millisecond time scale for *cis–trans* isomers [12] and a picosecond one for TICT-like effects [13]). The non-radiative relaxation induced transport term may be expressed as [3]

$$\left.\frac{\partial N(\Omega)}{\partial t}\right|_T = -\Phi \int \left(\frac{\partial N(\Omega_i)}{\partial t}\right)_{HB} P(\Omega_i \to \Omega)\, \mathrm{d}\Omega_i \tag{3}$$

in which Φ is the quantum yield for efficient re-orientation (non-radiative event) and $P(\Omega_i \to \Omega)$ is the probability of a transport from Ω_i to Ω. In the approximation of a free rotator, the free diffusion term may be expressed as

$$\left.\frac{\partial N(\Omega)}{\partial t}\right|_D = \underline{\underline{D}}\bar{\nabla}\bar{\nabla} N(\Omega) \tag{4}$$

in which D is the diffusion coefficient. A more realistic description would have to include restricted degrees of freedom [14], but this will not affect our conclusions.

Equations (2)–(4) are quite general ones and they lead to non-analytical solutions in the vast majority of cases. In order to describe simple practical situations, we recently treated extensively the case of linear molecules (DR1) excited with both linear and circular polarizations [9, 15]. For the purpose of an analytical development, we restrict ourselves here to the simplest case of linear molecules excited with linear polarizations. The optically driven rate equation for $N(\Omega)$ thus becomes [9]

$$\begin{aligned}\frac{\partial N(\Omega)}{\partial t} = &-\left(A\cos^2\theta + B\cos^4\theta + C\cos^3\theta\right)N(\Omega) \\ &+ \int \left(A\cos^2\theta_i + B\cos^4\theta_i + C\cos^3\theta_i\right)N(\Omega_i)\, P(\Omega_i \to \Omega)\, \mathrm{d}\Omega_i \\ &+ D\nabla^2 N(\Omega)\end{aligned} \tag{5}$$

in which the three elementary rates are displayed from top to bottom. θ in (5) is the angle between polarization and the molecule in the linear case. At this stage, the physics of the all-optical poling is clearer. Indeed, it was obvious that only the $\cos^3$ term in (5) bears polarity, but the two other $\cos^2\theta$ and $\cos^4\theta$ axial terms destroy the polarity, so that an optimum is found when the sum in brackets is a perfect square [16]. In a two-level system description, excitation factors are

$$\begin{aligned} A &\propto \mu_{01}^2 \left\| E_{2\omega}^2 \right\| \\ B &\propto \frac{\mu_{01}^2 \Delta\mu^2}{(2\hbar\omega)^2} \left\| E_{\omega}^4 \right\| \\ C &\propto \frac{\mu_{01}^2 \Delta\mu}{\hbar\omega} \left\| E_{\omega}^2 E_{2\omega}^* \right\| \cos(\Delta\Psi + \Delta k\, z) = 2\sqrt{AB}\cos(\Delta\Psi + \Delta k\, z) \end{aligned} \tag{6}$$

in which $\cos(\Delta\Psi + \Delta k\, z)$ is the self-quasi-phase-matching term [17], $\Delta k\, z$ is the projection of the wavevector mismatch on the propagation coordinate z and $\Delta\mu$ is the dipole moment difference between the ground and the excited state. We consider on optimal phase Ψ in the following, that is, $\cos(\Delta\Psi + \Delta k\, z) = 1$. Let us now make a further simplification in

equation (5). We do not have any physical insight into the orientation transport probability $P(\Omega_i \to \Omega)$. We thus assume that it is isotropic: $P(\Omega_i \to \Omega) = 1/4\pi$, which means that excited molecules relax with a random spherical orientation. With linear molecules moving freely in an isotropic medium, a non-random spherical orientation simply reduces Φ in (3). It cannot be as simple with octupolar molecules [18, 19] or with restricted rotators.

We can now solve equation (5). The writing process preserves symmetry around the polarization direction axis, so that the angular distribution $N(\Omega)$ depends only on the polar angle θ. In a weak orientation regime, we may write $N(\theta) = N_0 + N_1 \cos(\theta)$. Its evolution equation is

$$\begin{aligned} \frac{\mathrm{d}N_0}{\mathrm{d}t} &= 0 \\ \frac{\mathrm{d}N_1}{\mathrm{d}t} &= -(2D + 3A/4 + 5B/8)N_1 - (3C/4)N_0 \end{aligned} \tag{7}$$

in which N_0 is the total number of molecules. In the case of optimized seeding conditions with respect to the relative intensities, we have $A = B = C/2 \propto \mu_{01}^2 \| E_{2\omega}^2 \|$. We get the equation on the $\cos(\theta)$ term:

$$\frac{\mathrm{d}N_1}{\mathrm{d}t} = -(2D + 11A/8)N_1 - (3A/2)N_0 \tag{8}$$

whose solution describing $\chi^{(2)}$ growth is

$$N_1 = \frac{-12N_0A}{16D + 11A}\left[1 - \mathrm{e}^{-(2D+11A/8)t}\right]. \tag{9}$$

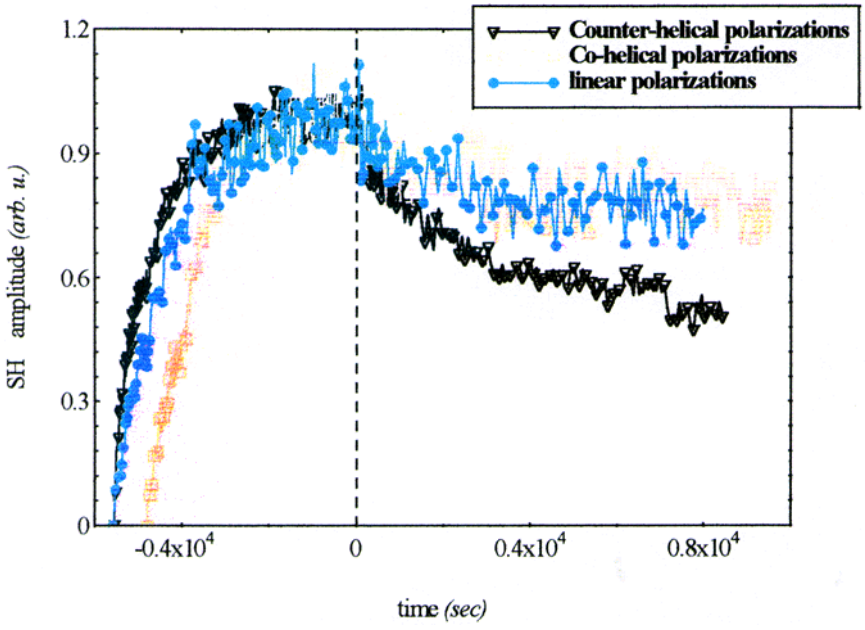

Figure 4. Real-time growth and decay of typical second-harmonic amplitudes ($\propto |\chi^{(2)}|$) in a PMMA–DR1 copolymer seeded at 1064 and 532 nm. Negative times correspond to the seeding preparation process. At time zero, the seeding process is stopped. Positive times correspond to $\chi^{(2)}$ decay.

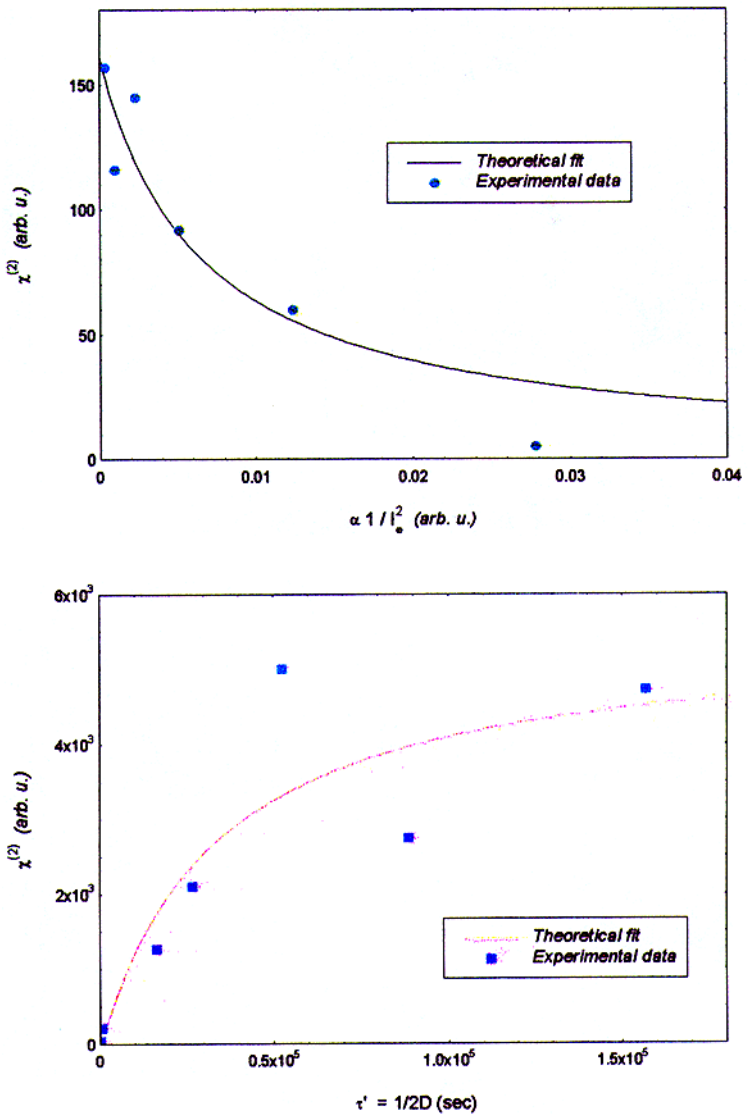

Figure 5. Influence of the fundamental beam energy expressed as I_{ω}^{-2} (top) and the seeding temperature expressed as $1/2D$ (bottom) on the maximum $\chi^{(2)}$ achieved. Samples were spin-coated thin films (0.3 μm) of the 35/65 PMMA–DR1 copolymer. In each case, experimental data correspond to optimized relative intensities and the relative phase for the seeding beams at ω and 2ω frequencies. The diffusion coefficient D is derived from $\chi^{(2)}$ experimental decay.

In this approximation the nonlinearity along the writing beam polarization direction is $\chi^{(2)} = N_1\beta/5\varepsilon_0$. Its maximum value which is achieved at the highest excitation rate A reaches $\chi^{(2)}_{\max} = -12N_0\beta/55\varepsilon_0$. After orientation, it decays as e^{-2Dt}. Only two parameters are involved in equation (9): the excitation rate A and the decay rate D. With the microscopic β value, we see that the all-optical poling process depends only

on three parameters when intensities and phase are optimized. The excitation rate is simply $A = \Phi\sigma I_{2\omega}\rho/2\hbar\omega$, in which Φ is the quantum yield for efficient reorientation after excitation, σ is the absorption cross section at 2ω, $I_{2\omega}$ is the laser intensity at 2ω and ρ is its duty cycle. ρ is defined as the product of the pulse duration and the repetition rate. It is $\rho \approx 10^{-9} \rightarrow 10^{-3}$ with pulsed picosecond YAG lasers.

3. All-optical poling dynamics: experiment

As described previously, the experiment consists in a seeding-type set-up [17]. The source was a Nd:YAG laser delivering 25 ps pulses at 1064 nm with a 10 Hz repetition rate. Writing and probing periods were alternated. Writing periods correspond to the simultaneous irradiation of the sample by the coherent superposition of the 1064 nm fundamental and the 532 nm second harmonic. The second harmonic is obtained by frequency doubling of the fundamental beam in a KDP crystal.

Typical $\chi^{(2)}$ rise and decay dynamics obtained with a PMMA-DR1 copolymer are given in figure 4. They correspond to optimal seeding conditions. Seeding with linear, co-helical and counter-helical ω and 2ω circular polarizations has also been checked [15]. Notice the similarity between the different growth and decay dynamics. Obviously, the different constants in (9) are symmetry dependent and they may be different for octupoles for instance [19]. Nevertheless, the model applies phenomenologically to all practical all-optical poling situations. Even the seeding of optical glass can be described with such a rate equation.

Experimentally, the diffusion constant D can be extracted from a fit to the decay at positive delays. It is then possible to check the dependence of the experimental $\chi^{(2)}$

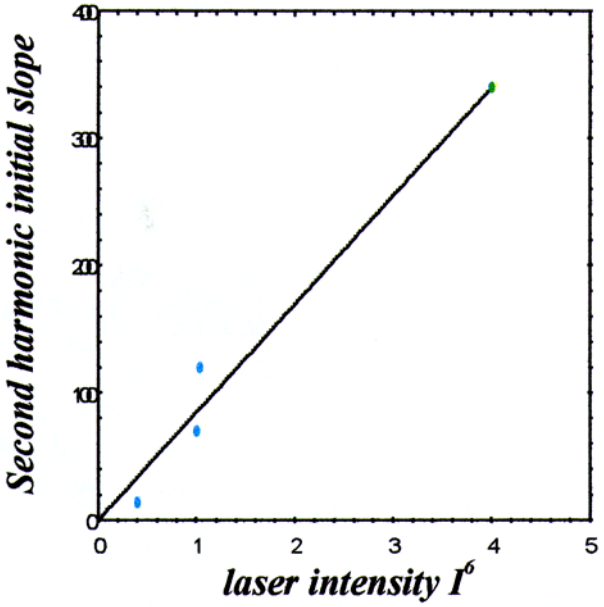

Figure 6. Dependence of the initial SH growth on the sixth power of the laser intensity in a PMMA–PAN rod.

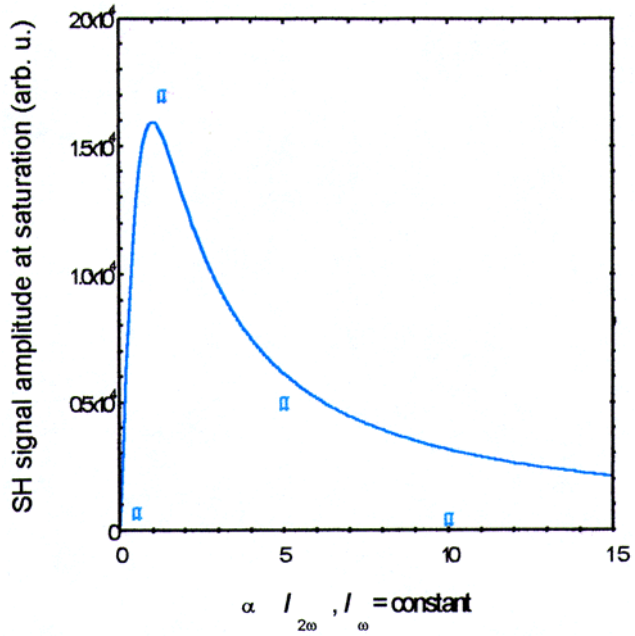

Figure 7. $I_{2\omega}$ laser intensity dependence of the SH signal amplitude induced at saturation in a PMMA–PNA rod, when I_{ω} is constant.

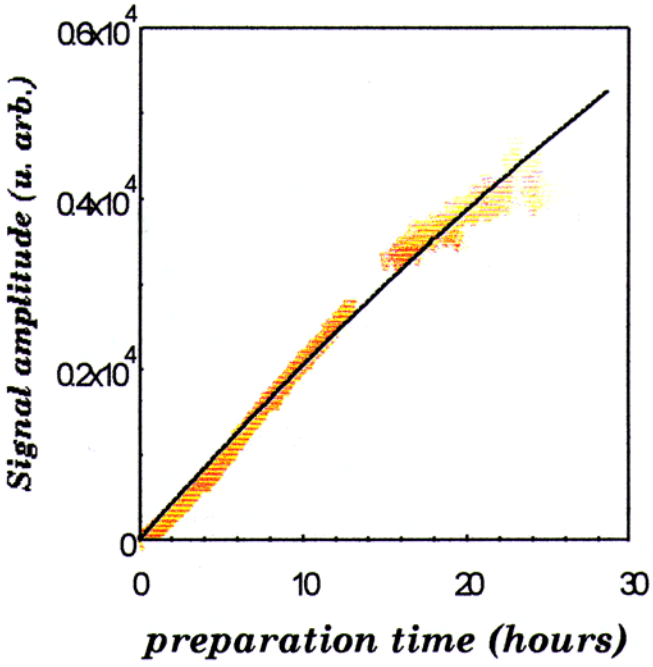

Figure 8. Time dependence of the induced SHG signal in a PMMA–PNA rod.

plateau on seeding intensity or temperature. Figure 5 shows the comparison between experimental and theoretical dependences derived from equation (9) in the case of parallel linear polarizations. Despite some scattering of the data owing to the difficulty of the experiment, the quality of the agreement demonstrates the validity and self-consistency of our description.

4. All-optical poling in a transparent polymer

Our model involves only β, A and D. In the case of a transparent polymer, the expression of A may be different. We performed all-optical poling at 1064/532 nm in PMMA–paranitroaniline (PNA) copolymer rods (5 mm thickness). Figure 6 represents the initial second-harmonic signal (SH) growth as a function of the sixth power of the laser beam I^6. We get $\mathrm{d}\left|\chi^{(2)}\right|^2/\mathrm{d}t \propto I_{2\omega} I_\omega^4$. In this polymer, we can express the excitation rate as $A = \Phi\,\delta I_\omega\, I_{2\omega}\rho/(\hbar\omega)^2$, in which δ is the two-photon absorption cross section of PNA.

In the same way as under resonant excitation, the relative fundamental and harmonic intensities can be optimized (cf figure 7). The time dependence of the SH growth is given in figure 8. At maximum signal, the green signal is visible with the naked eye. With 50% confidence, we get $\chi^{(2)} \approx 1$ fm V^{-1}, a value which is as low as in seeded optical glass [4]. The reason for such a low $\chi^{(2)}$-value may be found in the poor stability of the PNA orientation in PMMA. Indeed, PNA is a small molecule in comparison with DR1.

5. Conclusion

We have developed and resolved a simple model which clarifies the role of the different physical parameters on the all-optical poling dynamics. The model has been checked successfully using the intensity and temperature dependence of the $\chi^{(2)}$ induced in a PMMA–DR1 film under resonant excitation. Preliminary experiments on the all-optical poling of a transparent polymer have been presented. It shows that the principle can be extended to non-resonant materials in which phase-matching over large distances can be achieved [20]. We are far from the susceptibility $\chi^{(2)} = 150$ pm V^{-1} which could be induced in PMMA–DR1. However, orientation stability of PNA is poor in PMMA, and this dramatically reduces $\chi^{(2)}$, as our model predicts. This also shows that the *trans–cis* photoisomerization process, present in PMMA–DR1 and absent in PMMA–PNA, plays an important role in the efficiency of all-optical poling [21].

References

[1] Fiorini C, Nunzi J-M, Charra F and Raimond P 1996 *Opt. Photon. News* **7** 12
[2] Rochon P, Gosselin J, Natansohn A and Xie S 1992 *Appl. Phys. Lett.* **60** 4
[3] Sekkat Z and Dumont M 1992 *Appl. Phys.* B **54** 486
[4] Stolen R H and Tom H W K 1987 *Opt. Lett.* **12** 585
[5] Baranova N B and Zel'dovich B Ya 1987 *JETP Lett.* **45** 717
[6] Charra F, Devaux F, Nunzi J-M and Raimond P 1992 *Phys. Rev. Lett.* **68** 2440
[7] Fiorini C, Charra F and Nunzi J-M 1994 *J. Opt. Soc. Am.* B **11** 2347
[8] Charra F, Kajzar F, Nunzi J-M, Raimond P and Idiart E 1993 *Opt. Lett.* **18** 941
[9] Fiorini C, Charra F, Nunzi J-M and Raimond P 1997 *J. Opt. Soc. Am.* B **108** 1984
[10] Nunzi J-M, Charra F and Fiorini C 1993 *Condens. Matter News* **2** 6
[11] Nunzi J-M and Charra F 1992 *OSA Tech. Digests CLEO-QELS Conf. (Anaheim, CA)* paper JThC4

[12] Rau H 1989 *Photochemistry and Photophysics* vol 2, ed J F Rabek (Boca Raton, FL: Chemical Rubber Company) ch 4, p 119
[13] Lampre I, Marguet S, Markovitsi D, Delysse S and Nunzi J-M 1997 *Chem. Phys. Lett.* **212** 496
[14] Michelotti F Personal communication
[15] Etilé A-C, Fiorini C, Charra F and Nunzi J-M 1997 *Phys. Rev.* A **56** 3888
[16] Chalupczak W, Fiorini C, Charra F, Nunzi J-M and Raimond P 1996 *Opt. Commun.* **126** 103
[17] Fiorini C, Charra F, Nunzi J-M and Raimond P 1995 *Nonlin. Opt.* **9** 339
[18] Nunzi J-M, Charra F, Fiorini C and Zyss J 1993 *Chem. Phys. Lett.* **219** 349
[19] Fiorini C, Charra F, Nunzi J-M, Samuel I D W and Zyss J 1995 *Opt. Lett.* **20** 24
[20] Fiorini C, Nunzi J-M, Charra F, Kajzar F, Lequan M, Lequan R-M and Chane-Ching K 1997 *Chem. Phys. Lett.* **271** 335
[21] Charra F, Fiorini C, Kajzar F, Nunzi J-M, Raimond P and Chalupczak W 1996 *Photoactive Organic Materials. Science and Application* ed F Kajzar, V M Agranovich and C Y C Lee (Dordrecht: Kluwer) p 513